*Proc. Natl. Acad. Sci. USA*
Vol. 86, pp. 8753–8757, November 1989
Biophysics

# Photolysis of a photolabile precursor of ATP (caged ATP) induces microsecond rotational motions of myosin heads bound to actin

(muscle contraction/saturation-transfer EPR/molecular dynamics/spin label)

CHRISTOPHER L. BERGER, ERIC C. SVENSSON*, AND DAVID D. THOMAS†

Department of Biochemistry, University of Minnesota Medical School, Minneapolis, MN 55455

*Communicated by Hugh E. Huxley, July 10, 1989*

**ABSTRACT** **To test the proposal that ATPase activity is coupled to the rotation of muscle cross-bridges (myosin heads attached to actin), we have used saturation-transfer EPR to detect the rotational motion of spin-labeled myosin heads (subfragment 1; S1) bound to actin following the photolysis of caged ATP (a photoactivatable analog of ATP). In order to ensure that most of the heads were bound to actin in the presence of ATP, solutions contained high (200 μm) actin concentrations and were of low (36 mM) ionic strength. Sedimentation measurements indicated that 52 ± 2% of the spin-labeled heads were attached in the steady state of ATP hydrolysis during EPR measurements. Five millimolar caged ATP was added to the actin–S1 solution in an EPR cell in the dark, with no effect on the intense saturation-transfer EPR signal, implying a rigid actin–S1 complex. A laser pulse produced 1 mM ATP, which decreased the signal rapidly to a brief steady-state level that indicated only slightly less rotational mobility than that of free heads. After correcting for the fraction of free heads, we conclude that the bound heads have an effective rotational correlation time of 1.0 ± 0.3 μs, which is about 100 times shorter (faster) than that in the absence of ATP. To our knowledge, this is the first direct evidence that myosin heads undergo rotational motion when bound to actin during the ATPase cycle. It is likely that similar cross-bridge rotations occur during muscle contraction.**

Although the sliding filament theory of muscle contraction was proposed in 1954 (1, 2), the exact nature of the actin–myosin interactions that cause the filaments to slide past one another remains unclear. H. E. Huxley suggested in 1969 (3) that the most probable source of force generation is the rotation of the myosin head when bound to actin, and in 1971 A. F. Huxley and Simmons (4) proposed that the myosin head undergoes submillisecond rotations while bound to actin during isometric contraction. X-ray diffraction experiments on active muscle suggest that myosin heads remain in close proximity to actin during contraction (5), but there has been no direct evidence for the rotation of myosin heads bound to actin during the ATPase cycle.

Previous work on spin-labeled myosin heads in isometrically contracting muscle fibers, using conventional EPR to measure orientation (6) and saturation-transfer EPR (ST-EPR) to measure microsecond rotational motions (7), has shown that 80% of the heads are orientationally disordered and mobile on the microsecond time scale. One interpretation of these results is that the mobile heads are detached from the actin filament, but an alternative explanation is that they are bound to actin in a rotationally dynamic state. It is difficult to distinguish between these two possibilities in complex cycling systems as muscle fibers or myofibrils (8), since the fraction of attached heads is ambiguous. Although the stiffness of fibers in contraction is greater than 50% of the rigor value, whether labeled or not, stiffness is not necessarily a linear function of the fraction of attached heads (9). Microsecond rotational motions of spin-labeled myosin subfragment 1 (S1) crosslinked to actin in the presence of ATP have been observed by ST-EPR (10). However, it is not clear that the crosslinked heads are a true analog of noncovalently bound heads.

In the present study, in order to measure the ATP-induced motion of actin-attached spin-labeled S1 without crosslinking, we have performed ST-EPR on solutions containing high actin concentrations and of low ionic strength, which increases the affinity of spin-labeled myosin heads for actin (11). The principal advantage of using solutions of S1 and actin is the opportunity to make direct binding measurements, by using centrifugation, thus removing the ambiguity of attachment. However, the high ATPase activity of this preparation allows only a few seconds for EPR data acquisition. An ATP-regenerating system cannot be used, due to its high ionic strength, and rapid mixing is not feasible with such a viscous solution, due to EPR tuning problems. Therefore, we used the photolysis of the $P^3$-1-(2-nitrophenyl)ethyl ester of ATP (caged ATP), a photoactivatable analog of ATP (12), to rapidly produce millimolar concentrations of ATP in the sample during ST-EPR data acquisition. This still did not allow enough time to acquire the entire ST-EPR spectrum, so we monitored the intensity at one point in the center of the spectrum where the sensitivity to rotational motion is maximal (13). We thus measured the microsecond rotational motion of spin-labeled heads during the brief steady-state period of maximal activation by actin.

## MATERIALS AND METHODS

**Preparations.** Chymotryptic S1 was prepared as described previously (14), except that the chymotryptic digestion time was 10 min. F-actin was prepared as previously described (15). S1 was spin-labeled with 4-maleimido-2,2,6,6,-tetramethyl-1-piperinyloxy (MSL; Aldrich) to the extent of 0.98 ± 0.02 label bound per head, with a specificity of 1.00 ± 0.04 SH1 groups blocked per bound label, as previously described (10). Caged ATP was obtained from Calbiochem, and ATP was obtained from Sigma. Low ionic strength ($\mu$ = 36 mM) conditions are defined as 10 mM imidazole, 2 mM $MgCl_2$, 1 mM EGTA (pH 7.0) plus either 5 mM magnesium nucleotide (ATP or caged ATP) or 25 mM potassium propionate. Physiological ionic strength ($\mu$ = 186 mM) conditions were identical to low ionic strength conditions, except for the

The publication costs of this article were defrayed in part by page charge payment. This article must therefore be hereby marked "*advertisement*" in accordance with 18 U.S.C. §1734 solely to indicate this fact.

Abbreviations: S1, myosin subfragment 1; ST-EPR, saturation-transfer EPR; MSL, 4-maleimido-2,2,6,6,-tetramethyl-1-piperinyloxy; caged ATP, the $P^3$-1-(2-nitrophenyl)ethyl ester of ATP.

*Present address: Department of Biological Chemistry, University of California, Los Angeles, School of Medicine, Los Angeles, CA 90034.

†To whom reprint requests should be addressed.

addition of 150 mM potassium propionate. Hemoglobin was prepared and spin-labeled with MSL (MSL-hemoglobin) as previously described (13).

**Assays.** Protein concentrations were determined as described (15). The fraction of S1 bound to actin was measured by sedimenting 200 $\mu$l of 1 $\mu$M S1 and various concentrations of actin (10–200 $\mu$M), in the presence of 5 $Mg^{2+}$·ATP under low or physiological ionic strength conditions (as defined above) in a Beckman TL-100 centrifuge for 8 min at 386,000 $\times$ $g$ at 25°C. The $NH_4^+/Ca^{2+}$ ATPase activity (16) of the resulting supernatants containing unbound S1 was measured and compared with a zero-actin control to determine the amount of S1 bound to actin in the pellet. An actin-binding constant ($K_b$) was determined from the fraction of bound heads ($f_b$) under these conditions (Eq. 1) and used to determine the fraction of heads bound at the higher S1 concentrations used in ST-EPR experiments (Eq. 2).

$$K_b = [\text{actin–S1}]/[\text{actin}][\text{S1}] \quad [1]$$

and

$$f_b = [b - (b^2 - 4ac)^{1/2}]/2a, \quad [2]$$

where $a = K_b[\text{S1}]_{tot}$, $b = a + c + 1$, and $c = K_b[\text{actin}]_{tot}$.

The amount of caged ATP photolyzed in an experiment was determined by measuring the amount of inorganic phosphate produced as a result of hydrolysis by the S1 ATPase activity, using the method of Lanzetta *et al.* (17).

**EPR Experiments.** Steady-state ST-EPR spectra were obtained as described (13) with a Bruker ER200D spectrometer (IBM Instruments, Danbury, CT). Transient ST-EPR spectra were obtained at a single field position in the center of the spectrum, where the maximum intensity is observed for actin–MSL-S1 in the absence of ATP and where the sensitivity to rotational motion is maximal (13). To ensure that the transient EPR signal was always obtained at an equivalent spectral position, the ratio of the applied magnetic field to the microwave frequency was locked at a constant value by using the field/frequency lock of the spectrometer. The accuracy and reproducibility of this lock was verified by reference to the baseline-crossing points of 0.9 mM potassium nitrosodisulfonate (Alfa–Ventron, Danvers, MA) in 50 mM $K_2CO_3$. The samples were contained in a 50-$\mu$l fused silica flat cell (Wilmad Glass, Buena, NJ) and were maintained at a temperature of 25.0 ± 0.5°C by using a variable temperature controller (Bruker model ER4111 VT; IBM Instruments). Caged ATP was photolyzed during EPR experiments by using a 1-s burst (100 Hz) of 10-ns light pulses from an XeCl excimer laser (Lambda Physik model EMG53MSC; Acton, MA) at 308 nm. The light was directed by mirrors to pass through the radiation slits in the front of the cavity (Bruker $TE_{101}$; IBM Instruments). The front surface of the quartz dewar was roughened with diamond paste to ensure that the light intensity was uniform (±10%) over the entire sample, as verified with photosensitive film. Light energy incident on the sample, measured with a light meter connected to a fiber optic detector, was 20 ± 4 mJ/cm$^2$ for a standard 100-pulse burst. Approximately 0.1 s was required after the laser pulse for 1 mM caged ATP to be completely photolyzed. Recent improvements in sensitivity suggest that single-pulse experiments are feasible and that 10-ms time resolution is achievable.

**Spectroscopic Data Analysis.** All ST-EPR spectra were normalized by dividing by the double integral of the low-power ($H_1$ = 0.032 G) conventional EPR spectrum, obtained under equilibrium conditions (e.g., before caged ATP photolysis). This parameter is independent of rotational motion and corrects for any variation in the concentration of spin labels between the samples (13). In previous ST-EPR studies, spectra have been characterized by line-height ratios or spectral integrals that require information from more than one field position (13). However, in the present study involving transient signals, it was necessary to define a spectral parameter based on the intensity at a single field position. We chose to monitor the field position at which actin–MSL-S1 (no ATP) has its maximal ST-EPR spectral intensity, by using the field/frequency lock to ensure that the same field position was monitored in all experiments. The intensity at this position was normalized by dividing by the value obtained for actin–MSL-S1 (no ATP).

The effective rotational correlation time ($\tau_r$) values for MSL-hemoglobin, varied by changing the sample temperature and/or glycerol concentration, were calculated from the Stokes–Einstein–Debye equation for isotropic rotational diffusion: $\tau_r = V\eta/kT$, where $V$ = the molecular volume of the equivalent sphere (radius = 29 Å for hemoglobin), $\eta$ is the solution viscosity at a given temperature $T$, and $k$ is Boltzmann's constant (18). A plot of the normalized intensity values versus $\tau_r$, obtained from MSL-hemoglobin (Fig. 1), was used to determined $\tau_r$ in the caged ATP experiments. By using this intensity parameter, values of $\tau_r$ for actin–MSL-S1 in the absence of ATP (85 $\mu$s) and for free MSL-S1 (0.2 $\mu$s) from this parameter agreed with those obtained using the standard line-height ratio parameters. Although the effective correlation times determined by this procedure have high precision, they are probably not accurate estimates for the actual correlation times, since the motions of S1 are probably much more anisotropic than those of the hemoglobin model system.

The $\tau_r$ value for the bound heads during the steady-state S1 ATPase activity was obtained in the following manner. The ST-EPR spectral intensity for actin–MSL-S1 in the presence of saturating ATP is a linear combination of the intensity of bound heads and the intensity of free heads, weighted by their mole fractions:

$$I(\text{total}) = f_b \cdot I(\text{bound}) + (1 - f_b) \cdot I(\text{free}). \quad [3]$$

The fraction of bound heads ($f_b$) was determined directly from the centrifuge binding data, the normalized ST-EPR intensity of the free heads [$I$(free)] was determined from MSL-S1 in the absence of actin, and the normalized ST-EPR intensity of actin–MSL-S1 in the presence of saturating ATP [$I$(total)] was measured directly in the caged ATP experiment (defined as the briefly maintained steady-state intensity value obtained after photolysis of caged ATP). Thus the only

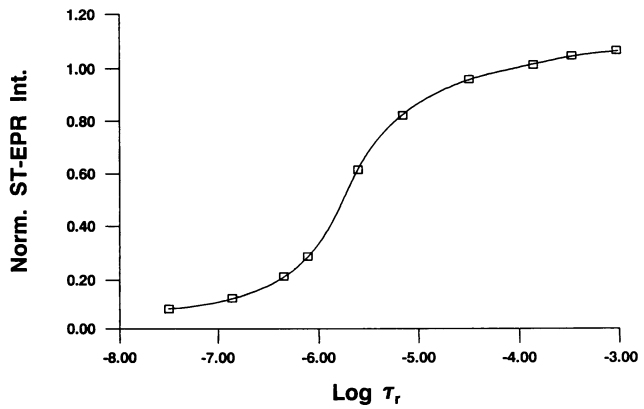


FIG. 1. Normalized ST-EPR intensity plotted as a function of the effective rotational correlation time ($\tau_r$), obtained from a series of spin-labeled hemoglobin samples with known correlation times. Intensity values are normalized to the intensity of actin–MSL-S1 in the absence of ATP ($\tau_r$ = 85 $\mu$s). This plot was used to determine the $\tau_r$ of the bound heads (Table 1, experiment 5).

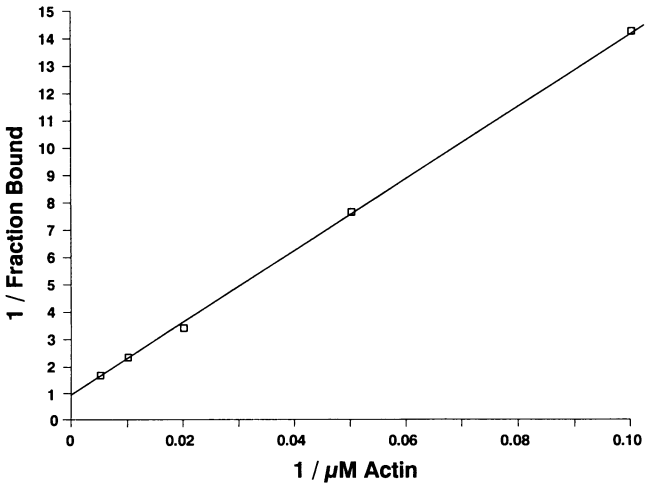


FIG. 2. Double-reciprocal plot of the fraction of myosin heads bound to actin at various actin concentrations. The fraction bound ($f_b$) was determined from sedimentation experiments. A binding constant of $K_b = 7.42 \pm 0.41 \times 10^3\ M^{-1}$ (mean ± SEM, $n = 12$) was determined (Eq. **1**) for MSL-S1 over a 10 μM to 200 μM range of actin concentrations. Samples contained 1 μM MSL-S1. The data were fitted by using linear regression analysis.

unknown in Eq. **3** is the normalized ST-EPR intensity of the bound heads [$I$(bound)], which can be determined by rearrangement of Eq. **3**:

$$I(\text{bound}) = [I(\text{total}) - (1 - f_b)\cdot I(\text{free})]/f_b. \quad [4]$$

## RESULTS

To determine unambiguously the fraction of attached heads in the presence of saturating ATP, centrifugation binding experiments were performed on solutions of actin and MSL-S1. In order to ensure that ATP was not depleted during the 8-min sedimentation, a low S1 concentration (1 μM) was used. The actin concentration was varied from 10 to 200 μM. The double-reciprocal plot of the fraction of bound heads versus actin concentration is linear (Fig. 2), and an actin-binding constant ($K_b$) of $7.42 \pm 0.41 \times 10^3\ M^{-1}$ (mean ± SEM, $n = 12$) was calculated from this data for MSL-S1 at 25°C in 5 mM ATP, 36 mM ionic strength at pH 7.0. This was not significantly different from the value obtained for unlabeled S1. $K_b$ was then used to determine that 52 ± 2% (Table 1, experiment 4) of the heads were attached to actin at low ionic strength in the presence of ATP under EPR conditions (100 μM MSL-S1 and 200 μM actin), where a greater concentration of MSL-S1 is required for signal intensity. No appreciable binding was observed in the presence of ATP at physiological ionic strength (Table 1, experiment 3). In the absence of ATP, essentially all of the labeled heads are bound to actin (Table 1, experiment 1), independent of ionic strength (36 mM to 186 mM), indicating normal rigor binding.

MSL-S1 is highly mobile on the submicrosecond time scale when free in solution (Fig. 3 *Left*), with $\tau_r = 0.2$ μs (Table 1, experiment 2). The ST-EPR spectrum of MSL-S1 is independent of ionic strength (36 mM to 186 mM) and the presence of ATP (10). The rotational motion of actin–MSL-S1 in the absence of ATP is slow on the microsecond time scale (Fig. 3 *Left*), with $\tau_r = 85$ μs (Table 1, experiment 1). This motion is entirely due to actin flexibility, since virtually identical ST-EPR spectra are obtained in the absence of ATP with solutions of MSL-actin and unlabeled S1 (15). Thus S1 is rigidly bound to actin in the absence of ATP, and MSL is rigidly bound to S1. The ST-EPR spectrum of actin–MSL-S1 is also independent of ionic strength (36 mM to 186 mM) in the absence of ATP. In the presence of ATP and an ATP regenerating system, the ST-EPR spectrum of actin–MSL-S1 at physiological ionic strength becomes identical to that of free MSL-S1 (10).

Photolysis of caged ATP was required to examine the rotational motions of actin–MSL-S1 in the presence of ATP at low ionic strength, since 5 mM ATP would be depleted in 1 min or less under EPR conditions, which is not enough time for mixing the viscous sample, putting it into the EPR cell, and tuning the spectrometer accurately. One minute still does not allow enough time for the acquisition of a full ST-EPR spectrum, so we monitored the intensity of a single field position in the center of the spectrum as a function of time before and after the photolysis of caged ATP. The ST-EPR spectra of actin–MSL-S1 and MSL-S1 are unaffected by the addition of caged ATP in the dark, as expected, since unphotolyzed caged ATP is not a substrate for myosin (12). Before the laser pulse, the ST-EPR intensity of actin–MSL-S1 is very high (Fig. 3), indicating that MSL-S1 is rigidly bound to actin. After the laser pulse, which produced 1–2 mM ATP, this intensity decreases (Fig. 3 *Right*), on the average, to 0.26 of its initial intensity (Table 1, experiment 4), implying increased microsecond rotational motion. At physiological ionic strength, the signal decreases to the free S1 level (0.16 of the initial intensity), as expected, since none of the S1 is bound to actin (Table 1, experiment 3). Thus, the motion seen at low ionic strength for actin–MSL-S1 is restricted compared to that of free S1 in the presence of ATP. Photolysis of caged ATP had no effect on the ST-EPR spectrum of S1 alone (Fig. 3 *Right*).

The ST-EPR spectral intensity of active heads in the presence of saturating ATP is a linear combination of the spectral intensity of the bound and free heads, weighted

Table 1. Fraction of bound heads, ST-EPR intensity, and effective rotational correlation times ($\tau_r$)

| Exp. | Complex (conditions) | Fraction bound* | ST-EPR intensity† | $\tau_r$, μs‡ |
|---|---|---|---|---|
| 1 | Actin–MSL-S1 (no ATP) | 0.99 ± 0.02 ($n$ = 5) | ≡1 | 8.5 ± 11 |
| 2 | MSL-S1 (no actin) | ≡0 | 0.16 ± 0.02 ($n$ = 8) | 0.2 ± 0.1 |
| 3 | Actin–MSL-S1 + ATP ($\mu$ = 186 mM) | 0.00 ± 0.03 ($n$ = 8) | 0.16 ± 0.01 ($n$ = 8) | 0.2 ± 0.1 |
| 4 | Actin–MSL-S1 + ATP ($\mu$ = 36 mM) | 0.52 ± 0.02 ($n$ = 12) | 0.26 ± 0.01 ($n$ = 8) | 0.5 ± 0.2 |
| 5 | Bound actin–MSL-S1 + ATP ($\mu$ = 36 mM)§ | ≡1 | 0.35 ± 0.03 | 1.0 ± 0.3 |

Values are the means ± SEM.

*The fraction of MSL-S1 bound to actin in EPR experiments was calculated (Eq. **2**) from the binding constants (Eq. **1**) determined in the sedimentation experiments (Fig. 2).

†The ST-EPR intensity was measured as described in *Materials and Methods* and the legend to Fig. 3.

‡Effective rotational correlation times ($\tau_r$) were calculated by using a plot of ST-EPR intensity vs. $\tau_r$, obtained from a series of spin-labeled hemoglobin samples having known correlation times (Fig. 1).

§The ST-EPR intensity was corrected for the measured fraction (0.48) of free heads (Eq. **4**), yielding a value for the ST-EPR intensity that corresponds directly to the bound heads. A $\tau_r$ value for the bound heads was then determined from this intensity value.

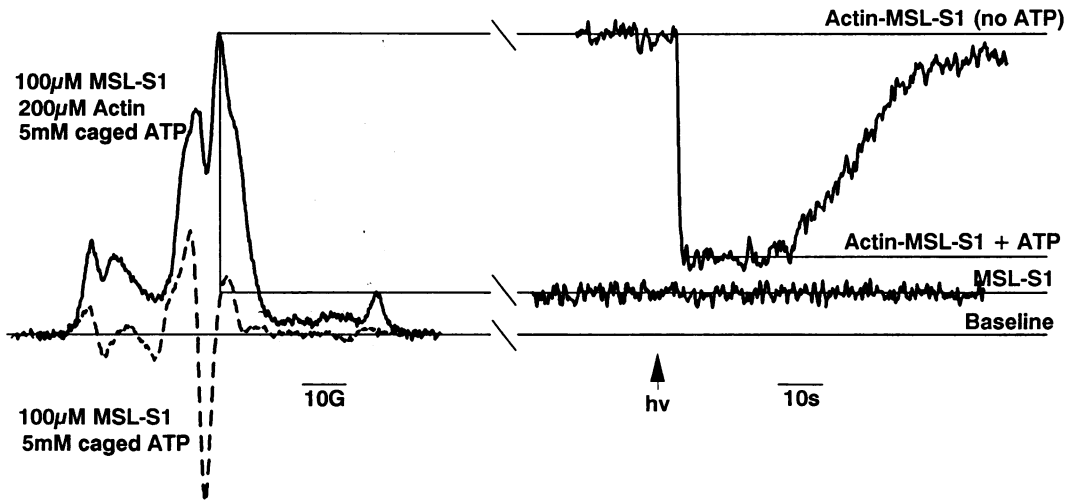


FIG. 3. Effect of the photolysis of caged ATP on the ST-EPR intensity of actin–MSL-S1 and MSL-S1 at low ionic strength ($\mu$ = 36 mM). (*Left*) ST-EPR spectra of 100 $\mu$M MSL-S1 with 200 $\mu$M actin (solid trace) and 100 $\mu$M MSL-S1 alone (dashed trace), in the presence of 5 mM caged ATP before photolysis, showing the spectral position at which the magnetic field was fixed. In the dark, these spectra were independent of caged ATP. Spectra were identical in the absence of caged ATP and/or at physiological ionic strength ($\mu$ = 186 mM). (*Right*) The spectral intensity at the fixed field position is plotted as a function of time. ATP (1–2 mM) was released in the sample at the laser pulse (arrow). The intensity of the actin–MSL-S1 solution (top trace) decreases rapidly to a steady-state level that is intermediate between that of rigor (no ATP) and free S1. Photolysis of caged ATP has no effect on the intensity of MSL-S1 alone (bottom trace).

respectively by their mole fractions (Eq. 3). So the ST-EPR intensity of the bound heads was calculated from Eq. 4 to be 0.35 of the initial intensity (Table 1, experiment 5). Therefore, from Fig. 1, $\tau_r$ for bound heads in the presence of saturating ATP is 1.0 ± 0.3 $\mu$s (Table 1, experiment 5).

Nonspecific effects of UV irradiation on our data are ruled out by the following results: The spectral trace recovers completely after the ATP is completely hydrolyzed by the actin–S1 (typically requiring about 2 min), and second exposure of the same sample to UV radiation produces the same change in the spectral trace. Glutathione, which is often used as a protective reagent in caged ATP experiments, cannot be used in EPR, since it destroys the EPR signal by reducing the spin label. Nevertheless, very little inhibition of ATPase activity was caused by flash photolysis: the actin-activated ATPase rate of the sample measured 5 min after caged ATP photolysis is 85 ± 10% of values before photolysis. Binding experiments with photolyzed caged ATP show MSL-S1 to have the same actin-binding affinity as with ATP. In addition, gel electrophoresis of irradiated samples indicates that UV-induced crosslinking of S1 to actin is not occurring.

## DISCUSSION

The observed increase in rotational motion upon photolysis of caged ATP (Fig. 3) is due not only to the detachment of heads in the presence of ATP but also to an increase in the rotational motion of the bound heads as well. The effective rotational correlation time ($\tau_r$) of 85 $\mu$s in the absence of ATP decreases to 1 $\mu$s in the presence of ATP for the bound heads. This value of $\tau_r$ is 5–10 times faster than that previously observed in the active myofibrils (8) or crosslinked actin–S1 (10). It is likely that heads in myofibrils are more restricted in their rotational motion due to their attachment to the myosin filament backbone, and the rotational motion of crosslinked actin–S1 may be more restricted due to the interprotein covalent crosslinks.

An alternative explanation is that the 1-$\mu$s rotational correlation time measured for the bound heads is actually a measure of a rapid association–dissociation reaction between S1 and actin. It is difficult to measure the dissociation rate for actin and S1 in the presence of ATP directly because it occurs at a rate of at least 500–1000 $s^{-1}$, well within the 2-ms dead time of most stopped-flow devices (19, 20). However, the second-order rate constant for the association of actin and S1 in the presence of ATP (at comparable temperature and ionic strength conditions) has been determined to be approximately $6 \times 10^6\ M^{-1}s^{-1}$ (19), and the equilibrium constant for the actin–S1 association reaction has been calculated to be approximately $1 \times 10^4\ M^{-1}$ (20). Therefore, the rate constant for the dissociation of S1 from actin in the presence of ATP at low ionic strength is between 500 and 1000 $s^{-1}$. Thus S1 and actin associate and dissociate on the millisecond time scale in the presence of ATP, which is much too slow to account for the observed 1-$\mu$s rotational correlation time of the bound heads. Since the exchange of the bound and the free S1 is much slower than the time scale for the spin-lattice relaxation (10 $\mu$s), the ST-EPR signals are a linear combination of the bound and free signals, so Eqs. 3 and 4 (see *Materials and Methods*) are valid (18).

The observed rotational motion could, in principle, be due to independent motions of the probe itself. However, previous experiments with MSL-S1 attached to glass beads show that MSL is rigidly attached to S1 ($\tau_r \geq 100$ $\mu$s) in the absence or presence of ATP (8). This motion could also be due to just one domain of the myosin head mobilizing in the presence of ATP while attached to actin. Experiments with other probes at different sites of the S1 molecule are necessary to test this possibility. It may also be that the flexibility of actin increases in the presence of S1 and ATP, which would increase the mobility of S1 under these conditions. This possibility could be examined with experiments using spin-labeled actin rather than S1.

The 1-$\mu$s effective rotational correlation time assumes a homogeneous population of bound heads in the presence of saturating ATP, all with the same $\tau_r$. However, considering the complexity of the actomyosin ATPase cycle, it is likely that these bound heads are a heterogeneous population with several different rotational correlation times. Time-resolved ST-EPR or phosphorescence will be necessary to resolve any heterogeneity in motion and to characterize these rotations precisely in terms of rates and amplitudes (21). Nevertheless, based on theoretical studies of ST-EPR (22), the large ATP-induced decrease in ST-EPR intensity implies that at least half of the attached myosin heads undergo rotational motions

with correlation times of 1 $\mu$s or less and amplitudes of 45° (full cone angle) or more.

It is unlikely that the observed binding at high actin concentrations is due to nonspecific trapping of the heads in the actin filament lattice. At 200 $\mu$M actin and physiological ionic strength, no appreciable binding is observed in the presence of ATP, showing that all of the S1 is dissociated from actin under these conditions (Table 1, experiment 3). The ST-EPR spectrum of actin–MSL-S1 in the presence of ATP at physiological ionic strength is identical to that of free S1, with a $\tau_r$ of 0.2 $\mu$s, showing that the presence of high actin concentrations has no effect on S1 mobility in the absence of binding. This is not surprising, since the total protein concentration in the EPR sample is about 20 mg/ml, which accounts for only 2% of the total solution volume. Thus, although the macroscopic viscosity of the solution, due to actin filament network, is high, the solution's microscopic viscosity is quite low, even at 200 $\mu$M actin. Furthermore, the actin-binding constant of MSL-S1 is independent of actin concentration from 10 $\mu$M to 200 $\mu$M (Fig. 2), indicating the affinity of S1 for actin is not altered at the higher actin concentrations. S1 binds independently to actin in the presence of adenylyl imidodiphosphate (AMPPNP), a nonhydrolyzable analog of ATP, at levels of up to 0.80 mole of S1 per mole of actin (23). Thus, the calculation of the fraction of bound heads (in the presence of ATP) at 100 $\mu$M MSL-S1 in the ST-EPR experiments, using the binding constant ($K_b$) measured from the sedimentation experiments at 1 $\mu$M MSL-S1, is valid.

While it is clear that SH1 modification perturbs the ATPase cycle of spin-labeled S1 through partial inhibition of the rate limiting step (24), binding to actin is not affected, and MSL-S1 is strongly activated by actin (10). Thus the essential conclusion of the present study, that attached heads have microsecond rotational motion during the steady state of the ATPase cycle, is almost certainly applicable to unlabeled myosin as well. Studies with higher time resolution or with ATP analogs will be necessary to deduce the rotational mobility of specific states in the biochemical mechanism. However, it is now clear that bound states in the ATPase cycle can have microsecond rotational mobility.

Our measurements of myosin head molecular dynamics are relevant to the recently developed *in vitro* movement assays, which have shown that S1 alone can produce both actin-filament movement (25) and force comparable to that produced in the muscle fiber (26). The sliding motions are so rapid that each actin monomer spends less than 1 ms in the vicinity of the S1 that is moving the filament, suggesting that submillisecond movements of S1 are required.

The existence of a dynamically bound state of S1 in the presence of ATP is very significant in the interpretation of previous EPR results on muscle fibers, in which most of the MSL-labeled myosin heads during an isometric contraction were found to be disordered (6) and mobile (7) on the microsecond time scale. In light of the results presented here, it is likely that much of the disordered mobile population of myosin heads may actually be attached during contraction in the muscle fiber, as suggested by Huxley and Kress (27). This study provides direct evidence for the rotational motion of attached myosin heads on actin during the ATPase cycle, and attached cross-bridges in the muscle fiber are likely to undergo similar (but probably more restricted) motions during contraction.

We thank John Matta, Richard Stein, and Piotr Fajer for helpful discussions and also Sandra Johnson, Robert Bennett, and Ben Etzkorn for technical assistance. This work was supported by grants from the National Institutes of Health (AR32961 and AR39754), the Muscular Dystrophy Association of America, and the Minnesota Supercomputer Institute. D.T.T. was supported by an Established Investigatorship from the American Heart Association. C.L.B. was supported by a Training Grant from the National Institutes of Health.

1. Huxley, H. E. & Hanson, J. (1954) *Nature (London)* **173,** 973–976.
2. Huxley, A. F. & Niedergerke, R. (1954) *Nature (London)* **173,** 971–973.
3. Huxley, H. E. (1969) *Science* **114,** 1356–1366.
4. Huxley, A. F. & Simmons, R. M. (1971) *Nature (London)* **233,** 533–538.
5. Haselgrove, J. C. & Huxley, H. E. (1973) *J. Mol. Biol.* **77,** 549–568.
6. Cooke, R., Crowder, M. S. & Thomas, D. D. (1982) *Nature (London)* **300,** 776–778.
7. Barnett, V. A. & Thomas, D. D. (1989) *Biophys. J.* **56,** 517–523.
8. Thomas, D. D., Ishiwata, S., Seidel, J. C. & Gergely, J. (1980) *Biophys. J.* **32,** 873–890.
9. Pate, E. & Cooke, R. (1988) *Biophys. J.* **53,** 561–573.
10. Svensson, E. C. & Thomas, D. D. (1986) *Biophys. J.* **50,** 999–1002.
11. Brenner, B., Schoenberg, M., Chalovich, J. M., Greene, L. E. & Eisenberg, E. (1982) *Proc. Natl. Acad. Sci. USA* **79,** 7288–7291.
12. McCray, J. A., Herbette, L., Kihara, T. & Trentham, D. R. (1980) *Proc. Natl. Acad. Sci. USA* **77,** 7237–7241.
13. Squier, T. C. & Thomas, D. D. (1986) *Biophys. J.* **49,** 921–935.
14. Eads, T. M., Thomas, D. D. & Austin, R. H. (1984) *J. Mol. Biol.* **179,** 55–81.
15. Thomas, D. D., Seidel, J. C. & Gergely, J. (1979) *J. Mol. Biol.* **132,** 257–273.
16. Chalovich, J. M. & Eisenberg, E. (1982) *J. Biol. Chem.* **257,** 2432–2437.
17. Lanzetta, P. A., Alvarez, L. J., Reinach, P. S. & Candia, O. A. (1979) *Anal. Biochem.* **100,** 95–97.
18. Thomas, D. D., Dalton, L. R. & Hyde, J. S. (1976) *J. Chem. Phys.* **65,** 3006–3024.
19. White, H. D. & Taylor, E. W. (1976) *Biochemistry* **15,** 5818–5826.
20. Stein, L. A., Schwarz, R. P., Chock, P. B. & Eisenberg, E. (1979) *Biochemistry* **18,** 3895–3909.
21. Thomas, D. D. (1986) in *Techniques for the Analysis of Membrane Proteins*, eds. Ragan, C. I. & Cherry, R. J. (Chapman & Hall, London), pp. 377–421.
22. Thomas, D. D., Eads, T. M., Barnett, V. A., Lindahl, K. M., Momont, D. A. & Squier, T. C. (1985) in *Spectroscopy and the Dynamics of Molecular Biological Systems*, eds. Bayley, P. M. & Dale, R. E. (Academic, London), pp. 239–257.
23. Greene, L. E. & Eisenberg, E. (1978) *Proc. Natl. Acad. Sci. USA* **75,** 54–58.
24. Mulhern, S. A. & Eisenberg, E. (1978) *Biochemistry* **17,** 4419–4425.
25. Toyoshima, Y. Y., Kron, S. J., McNally, E. M., Niebling, K. R., Toyoshima, C. & Spudich, J. A. (1987) *Nature (London)* **328,** 537–539.
26. Kishino, A. & Yanagida, T. (1988) *Nature (London)* **334,** 74–76.
27. Huxley, H. E. & Kress, M. (1985) *J. Muscle Res. Cell Motil.* **6,** 153–162.